NASA-TMX-72532

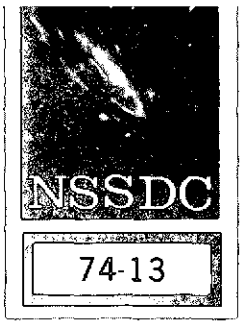

Comparison of the Trapped Electron Models AE-4 and AE-5 with AE-2 and AE-3

SEPTEMBER 1974

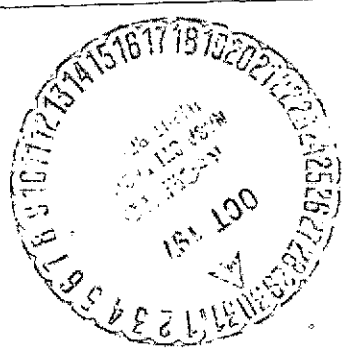

NATIONAL SPACE SCIENCE DATA CENTER

NATIONAL AERONAUTICS AND SPACE ADMINISTRATION • GODDARD SPACE FLIGHT CENTER, GREENBELT, MD.

NSSDC 74-13

COMPARISON OF THE TRAPPED ELECTRON MODELS AE-4 AND AE-5 WITH AE-2 AND AE-3

By

Robert H. Hilberg
Michael J. Teague
James I. Vette

Technical Editor

Margaret L. King

National Space Science Data Center
National Aeronautics and Space Administration
Goddard Space Flight Center
Greenbelt, Maryland 20771

September 1974

CONTENTS

		Page
1.	INTRODUCTION	1
2.	GENERAL CHARACTERISTICS	3
3.	DEPENDENCE ON L	7
4.	DEPENDENCE ON B	9
5.	ENERGY SPECTRUM	13
6.	LOCAL TIME DEPENDENCE	15
7.	STATISTICAL MODEL	17
8.	ORBIT INTEGRATIONS	19
REFERENCES		21

ILLUSTRATIONS

Figure		Page
1	Radial Profile of Omnidirectional Equatorial Flux of Electrons with Energies Above 0.04 MeV Near Solar Minimum	23
2	Radial Profile of Omnidirectional Equatorial Flux of Electrons with Energies Above 0.5 MeV Near Solar Minimum	24
3	Radial Profile of Omnidirectional Equatorial Flux of Electrons with Energies Above 2 MeV Near Solar Minimum	25
4	Radial Profile of Omnidirectional Equatorial Flux of Electrons with Energies Above 0.04 MeV Near Solar Maximum	26

CONTENTS (continued)

Figure		Page
5	Radial Profile of Omnidirectional Equatorial Flux of Electrons with Energies Above 0.5 MeV Near Solar Maximum	27
6	Radial Profile of Omnidirectional Equatorial Flux of Electrons with Energies Above 2 MeV Near Solar Maximum	28
7	Comparison of the Cutoff Magnetic Field Used in AE-4 and AE-5 with AE-2 as a Function of L	29
8	Dependence of Omnidirectional Electron Flux on Magnetic Field Intensity for L = 1.5 Earth Radii	30
9	Dependence of Omnidirectional Electron Flux on Magnetic Field Intensity for L = 3.0 Earth Radii	31
10a	Dependence of Omnidirectional Electron Flux on Magnetic Field Intensity for L = 5.0 Earth Radii for AE-2 and AE-4	32
10b	AE-4 Dependence of Omnidirectional Electron Flux on Magnetic Field Intensity for L = 5.0 Earth Radii	32
11	Equatorial Omnidirectional Integral Spectrum of Electrons at L = 1.5 Earth Radii, Normalized to Unity at 0.5 MeV	33
12	Equatorial Omnidirectional Integral Spectrum of Electrons at L = 3.0 Earth Radii, Normalized to Unity at 0.5 MeV	34
13	Equatorial Omnidirectional Integral Spectrum of Electrons at L = 5.0 Earth Radii, Normalized to Unity at 0.5 MeV	35

CONTENTS (continued)

Figure		Page
14	Equatorial Omnidirectional Integral Spectrum of Electrons at L = 6.6 and 6.0 Earth Radii, Normalized to Unity at 0.5 MeV	36
15	Local Time Dependence of Flux for AE-3 at L = 6.6 Earth Radii and AE-4 at L = 6.5 Earth Radii	37
16	Standard Deviation for Log-Normal Statistical Functions for AE-3 at L = 6.6 Earth Radii and AE-4 at L = 6.5 Earth Radii	38
17	Comparison of Orbit Integrations for 50 keV Electrons Near Solar Minimum	39
18	Comparison of Orbit Integrations for 0.5 MeV Electrons Near Solar Minimum	40
19	Comparison of Orbit Integrations for 2 MeV Electrons Near Solar Minimum	41
20	Comparison of Orbit Integrations for 50 keV Electrons Near Solar Maximum	42
21	Comparison of Orbit Integrations for 0.5 MeV Electrons Near Solar Maximum	43
22	Comparison of Orbit Integrations for 2 MeV Electrons Near Solar Maximum	44

1. INTRODUCTION

With the development of the AE-4[1] and AE-5[2, 3] models of geomagnetically trapped electrons, the AE-2[4] and AE-3[5] models have been superseded. Since these older models have been in use for many years and many calculations have been performed to predict mission fluxes using them, a comparison of these models to describe how the use of the latest models will change flux estimates is essential.

The differences in the model environments have been caused by a change in both the existing environment and the available data from which the models were derived. Different data analysis techniques have also influenced the models.

All of the models except AE-3 presented omnidirectional integral flux as a function of L shell, the magnetic field intensity B, and the energy E. Since AE-3 gives fluxes only for the synchronous altitude L = 6.6 Earth radii, no L dependence is contained in this model. In addition, models AE-3 and AE-4 included functions describing the local time dependence and the statistical time variation due to the effects of magnetic storm activity. This document compares the dependence of the flux on each of the relevant variables. Section 2 describes the general characteristics of the models; Section 3 shows the radial profiles of the models; Section 4 discusses the dependence of the flux on B; Section 5 presents the dependence of the flux on energy; Section 6 compares the AE-3 and AE-4 dependence of flux on local time, or longitude with respect to the Earth-Sun line; and Section 7 describes the statistical models of AE-3 and AE-4. To show the effects of these model differences, Section 8 includes a comparison of orbital flux integrations for a range of orbits.

2. GENERAL CHARACTERISTICS

The flux of electrons encountered in space is a function of B, L, E, local time, and universal time. Several factors are to be considered when evaluating the temporal variation of the flux. The Starfish event occurred in July 1962, masking the natural electron flux to varying degrees in the inner zone up to 1970[6]. These electrons were lost from the trapping region in a continuous fashion. Superimposed on the loss of Starfish electrons is the effect of the varying frequency of magnetic storms over the solar cycle on electron populations. In practice, models have been made for solar maximum and solar minimum since it is impossible within the accuracy and completeness of the data to infer intermediate conditions. The effect of large individual magnetic storms is treated differently in the inner and outer zones. In the inner zone the effects of storms are observed only for higher L values and then on an infrequent basis; during such times the flux changes are substantial. In the outer zone many storms, from small to large, cause such highly variable fluxes that a statistical model has been adopted. Rapid radial diffusion and fast loss mechanisms contribute to this variability.

The AE-2 model represents the situation in August 1964 and includes data collected primarily before that time. At that epoch the inner-zone flux for $L < 2.0$ Earth radii was dominated by Starfish electrons. This period occurred near the minimum of the solar cycle. A version of AE-2 was developed for epoch December 1968 near solar maximum. To extrapolate to this epoch from the data taken through 1964, both Starfish electron loss and the effects of the solar cycle were estimated. Both Starfish decay rates and duration of decay were estimated and the 1964 model flux reduced appropriately. To include the effects of the solar cycle, the outer-zone intensitites were increased and the peaks of the radiation zone moved to lower L values. Analysis of data available for AE-4 proved these extrapolations to be quite erroneous.

The AE-3 model gives values for both solar minimum and maximum at L = 6.6 Earth radii. The functional forms of the B, E, and local time dependences are the same for the two periods, but the absolute intensity is twice as high at solar minimum, and the estimated error is of the same magnitude.

The AE-4 model is presented for two epochs, 1964 and 1967. Data from both of these epochs were available for the development of the models. Since Starfish fluxes did not affect the outer zone, these models should be representative of the periods near solar minimum and maximum for any solar cycle with equivalent magnetic substorms.

The AE-5 model consists of versions for both the epochs 1967 and 1975. The AE-5 epoch 1967 model includes data influenced by Starfish fluxes. Attempts were made to separate Starfish fluxes from natural fluxes. This natural flux was then extrapolated to the 1975 solar minimum period. The accuracy of this procedure can only be evaluated when data from this epoch are available, since previous solar minimum data have been strongly influenced by Starfish electrons. The 1967 AE-5 model should be representative of solar maximum conditions except in the cases where Starfish electrons were still important ($L < 1.6$ Earth radii and $E > 500$ keV approximately).

AE-2 does not specifically treat the variations of flux levels accompanying geomagnetic activity. Further, the flux levels given are representative of the average of the logarithm of the flux since only crude statistical techniques were employed in its construction. AE-3 and AE-4 use a more sophisticated statistical model that gives the probability of exceeding a given flux level by fitting the flux variations to a log-normal distribution. Values of the average flux and the standard deviation, σ, are given in these models. The average flux is related to the average of the logarithm of the flux by the factor $10^{1.15\sigma^2}$.[1]

In all of the models except AE-3, the omnidirectional integral equatorial flux is given as a function of L. AE-3 represents conditions only at L = 6.6 Earth radii, and only a geometrical interpretation of L, as opposed to a physical one, is used. This function is multiplied by other functions evaluating the dependence of flux on B, E, and local time. While these functions are not explicitly identified in the computer forms of the AE-4 and AE-5 models, they represent a reasonable means for separating the various dependences in this comparison.

The following comments regarding these functional forms and the assumptions behind them should be noted. All models except AE-5 treat the B dependence as independent of energy. AE-3, AE-4, and AE-5 use analytic functions to represent the B dependence. AE-3 and AE-4, the two models in which the flux is a function of local time, use analytic representations to show this dependence. In both models the local time function depends on energy.

In AE-2 and AE-3 the energy spectrum is representated by an exponential form, although for AE-2 the exponential parameter is energy dependent for energies less than 2.5 MeV. For AE-3 the spectrum changes from an exponential form because of the effects of the local time function and is a pure exponential only at local noon.

The accuracy of the various models depends on the point in B, L, E space under consideration. In no case is the estimated accuracy of a model better than about a factor of 2. In "The Inner Zone Electron Model AE-5,"[2] an effort is made to use confidence codes to represent expected model accuracy of AE-5. These codes range from 1 to 10 and correspond to a model accuracy of a factor of 2 to a factor in excess of 10.

3. DEPENDENCE ON L

The omnidirectional integral equatorial fluxes for threshold energies 0.04 MeV, 0.5 MeV, and 2 MeV are given in Figures 1, 2, and 3 for the solar minimum period. In the inner zone the estimated Starfish flux for October 1964 has been added to the AE-5 flux for comparison with the AE-2 model, since AE-2 included both natural and Starfish electrons. At all energies, the agreement in the inner zone ($L \leq 2.4$ Earth radii) is good.

In the outer zone the AE-4 flux curves are consistently higher than AE-2, especially for L above 5 Earth radii. Part of this difference is caused by the fact that AE-2 represents an average of the logarithm of the flux, which amounts to about a factor of 2 in most cases. When the AE-2 curves are raised appropriately, reasonable agreement is obtained except for the following regions. For 40 keV electrons AE-2 is too low for L above 5 Earth radii. For 500 keV electrons AE-2 is too low in the slot (L in the range 2.2 to 3.5 Earth radii) and for L above 5 Earth radii. For 2 MeV electrons AE-2 is too low for L above 4.5 Earth radii.

The divergence of these models above L = 5 Earth radii is caused in part by the fact that AE-2 did not model the local time dependence, coupled with the use of the average of the logarithm of the flux. The effective averaging over local time performed in AE-2 using the logarithm of the flux produced a value about 10-20 percent lower for L = 6 Earth radii than an average of the fluxes would have produced. Further, the statistical variation at L = 6 Earth radii would have given an average flux another factor of approximately 2 higher, depending on the energy.

In addition, in the development of AE-4 a more complete set of data was available from the electron spectrometers on OGO 1 and OGO 3. Therefore, these data were given greater emphasis in determining absolute flux levels, while in AE-2 the Explorer 14 data were emphasized more.

Curves showing the omnidirectional integral equatorial fluxes above 0.04 MeV, 0.5 MeV, and 2 MeV for the solar maximum period are shown in Figures 4, 5, and 6. Both the 0.04 MeV and 0.5 MeV curves show that in extrapolating to solar maximum from 1964, the peak of the inner zone, which was dominated in 1964 by Starfish electrons, was not permitted to decay long enough. This choice was influenced by some unpublished Explorer 4 electron data. For 2 MeV electrons AE-2 carried this decay too long, so that the AE-2 flux was too low. At all energies the slot and the peak in the outer zone were pushed to excessively low L values, and the peak in the outer zone was too high. This choice was based on Explorer 6 data.

4. DEPENDENCE ON B

The B dependence of the electron flux refers to the decrease in flux intensity as one follows a dipole field line from the equator to lower altitudes. Since these functions are normalized to unity at the equator, the important variables are the shape of the curves and the cutoff B value, or the B value above which the flux can be considered to be zero. In all models the dependence on B was treated as independent of time, so that the same function was used for solar minimum and solar maximum forms of a given model. Therefore, the models will be compared in detail in their solar minimum forms, and data comparisons for this epoch will be made.

The cutoff B values were determined in AE-4 in a fashion different from the other models. AE-2 determined the cutoff by analyzing the data for low altitudes. The cutoff in AE-5 was determined in the same way for $L < 1.7$ Earth radii, but for $L \geq 1.7$ Earth radii the cutoff value was determined by the relationship $B_c = 0.16 + 0.06L$ gauss. This relationship was based on restricting the minimum mirroring altitude to which a particle would travel as it drifted around the Earth to a value $h_{min} = 100$ km. In AE-4 the decision was made to represent a conservative estimate of the flux. This led to the constraint on the mirroring altitudes that $h_{max} = 200$ km (discussed as follows).

The cutoff B values are shown in Figure 7 as a function of L. The AE-2 values agree with AE-5 at all L values and with AE-4 for L greater than 4 Earth radii. However, in the slot region and inner part of the outer zone, L in the range 2.5 to 4 Earth radii, the AE-4 model cuts off at much larger B values than AE-2. The effect of this difference is that in the range $2.5 \leq L < 4$ Earth radii, there is a large region of high B values at which AE-2 predicts no flux and AE-4 predicts a finite flux. Since neither model employs a longitudinal effect, the choice is somewhat a matter of taste. In AE-4 preference was given to showing a finite flux where electrons had been observed at the expense of predicting a flux

where it was known at certain longitudes (for a given B, L) that no fluxes had ever been observed. In contrast AE-2 gave a zero flux at points where electrons had been observed at low altitudes.

In Figure 8 the dependence of flux on B is shown for L = 1.5 Earth radii and E = 0.5 MeV. The agreement here is quite good. This L value was chosen because it is near the peak of the inner belt, but good agreement is seen throughout the inner zone. Differences that are seen here arise in part from the fact that the pitch angle distribution functions for Starfish and naturally occurring electrons are somewhat different.

Figure 9 shows curves comparing AE-2 and AE-4 at L = 3 Earth radii, the heart of the slot region. The curves are quite different for B greater than 0.3 gauss, and this type of difference can be expected from the difference in definition of cutoff used in the two models. This situation will be discussed further with the rest of the outer zone.

Throughout the outer zone the AE-2 and AE-4 flux-B functions are markedly different, even for L $\geq$ 4 Earth radii where the cutoff B values are the same for the two models. Figure 10a shows the situation at L = 5 Earth radii near the peak of the outer zone. The difference in shapes is caused largely by the differences in the equatorial flux levels that are assumed. The AE-4 distribution, G, was determined by a fit of the function

$$G = (B/B_o)^{-m} \left(\frac{B_c - B}{B_c - B_o}\right)^{m+1/2} \qquad B \leq B_c$$

$$= 0 \qquad B > B_c$$

where B_o is the equatorial B value and B_c the cutoff value. The data sets that were used in AE-4 measured fluxes relatively close to the equator, and Explorer 14 data that contributed to the fit are shown in Figure 10a.

The cutoff region in AE-2 is determined from the INJUN 3 data shown in the figure. When the renormalization of the AE-2 equatorial flux based on the difference between AE-2 and AE-4 is considered, the INJUN 3 data appear as shown in Figure 10b. Clearly, the INJUN 3 and AE-4 data agree within the experimental scatter shown for the Explorer 14 channels. Therefore, the shape of the AE-2 B dependence is felt to be incorrect because of the low value of the equatorial flux that was adopted.

The B dependence is a function of m and B_c for $L \geq 3$ Earth radii. Because of the smooth fit with the inner zone model in the slot region, these parameters have a strong influence in the range $2.4 < L < 3$ Earth radii. The parameter m is determined largely by data collected at low latitudes. On the other hand, high B data with adequate statistical coverage were not available for AE-4, so that B_c could not be determined strictly from the data but had to be specified by some external condition. The condition used was $h_{max} = 200$ km.

5. ENERGY SPECTRUM

The spectral functions of the new models agree reasonably well with the old ones at lower energies, but at high energies there are significant differences. It should be emphasized that these high-energy regions are based largely on extrapolation since accurate high-energy measurements (e.g., 5 MeV) were difficult to make. Those threshold detectors with adequate geometric factors were not calibrated accurately, and the spectrometer instruments did not reach these energies. The AE-2 spectra are simple exponential forms for energies greater than 2.5 MeV, and in all cases this spectrum gives higher fluxes above approximately 4 MeV than AE-4 or AE-5.

Figure 11 shows AE-2 and AE-5 integral spectral at L = 1.5 Earth radii. For energies greater than 2 MeV, AE-2 gives increasingly higher flux relative to AE-5. Two factors are involved here. AE-2 includes Starfish electrons that have a much harder spectrum than naturally occurring electrons. The development of AE-5 included no data for electrons with energies above 2.3 MeV (the upper limit measured by Vampola's electron spectrometer on OV3-3), so that the shape of the curve above this energy is largely an estimate.

Figures 12 and 13 compare the AE-2 and AE-4 integral spectra at L = 3.0 and 5.0 Earth radii, respectively. Again, AE-2 becomes much higher relative to AE-4 for energies greater than about 4 MeV. Since the highest threshold energy available for the development of AE-4 was about 4.5 MeV (McIlwain's electron-proton detector on Explorer 26), these differences result from the extrapolation technique.

Figure 14 shows the spectrum, normalized to unity at 0.5 MeV, given by AE-3 and AE-4 at L = 6.6 Earth radii and by AE-2 at L = 6.0 Earth radii. Both AE-2 and AE-3 spectra appear too soft for intermediate energies.

6. LOCAL TIME DEPENDENCE

The interaction of the solar wind with the magnetosphere produces external current sources that distort the geomagnetic field for L greater than about 5 Earth radii, so that B and L are not an adequate coordinate system for ordering the particle data. Therefore, a third coordinate has been introduced in AE-3 and AE-4 to account for this distortion. This variable is local time and represents a longitude with respect to the Earth-Sun line.

Figure 15 shows the local time functions from AE-3 at L = 6.6 Earth radii and AE-4 at L = 6.5 Earth radii for 40 keV, 0.5 MeV, and 2 MeV. Both the amplitudes of the variations and the shapes of the curves are different. However, in evaluating these differences, remember that the AE-3 curves were based on data from spacecraft with elliptical orbits, with relatively few passages through the region of interest. AE-4, on the other hand, had available data collected by ATS 1, which was in circular orbit at L = 6.6 Earth radii and provided vastly superior statistics.

7. STATISTICAL MODEL

In the outer electron zone, flux levels change frequently with large amplitude because of varying magnetic activity. To describe this variation a statistical model has been adopted in AE-3 and AE-4. This model evaluates the probability that the observed intensity will exceed a specified value by a given amount. In both of these models the statistical function took the form of the normal distribution with the variable being the logarithm of the flux.

The standard deviation for these models is shown in Figure 16. Agreement is reasonably good in the region 80 keV $\leq$ E $\leq$ 2 MeV where data coverage is best. Again, the data available for inclusion in AE-4 were more extensive than for AE-3.

8. ORBIT INTEGRATIONS

To evaluate the overall results produced by the differences between the new models and the old ones, several plots have been included showing orbit-integrated fluxes for a range of circular orbits with inclinations of 30 degrees and 90 degrees. Figure 17 shows orbit-integrated fluxes of 50 keV electrons at solar minimum, and Figures 18 and 19 show corresponding curves for 0.5 MeV and 2 MeV. Figures 20, 21, and 22 show corresponding curves for the period around solar maximum.

At solar minimum, major differences occur at the peak of the inner zone where Starfish electrons elevate the AE-2 flux and in the region above the outer zone peak. The rapid falloff of AE-2 relative to AE-4 for altitudes above 12,000 km results from the fact that AE-2 falls off faster than AE-4 and the AE-2 flux cuts off at L = 6 Earth radii.

At solar maximum the shapes of the curves are quite different, and factor-of-five differences are not uncommon. In general the agreement at solar minimum is much better than at solar maximum where extrapolation led to significant errors not always in the conservative direction.

The largest differences are seen for high energies, particularly in the slot and outer zone, so that the largest changes produced by calculating orbit fluxes using the new models occur in missions that spend large fractions of their time in these regions. However, for applications where very high energy electrons are not a factor, and where the time spent in the altitude region between about 12,000 n.m. and the limit of stable trapping is small, differences of less than an order of magnitude arise when Starfish decay is included in the calculations.

REFERENCES

1. G. Wayne Singley and James I. Vette, "The AE-4 Model of the Outer Radiation Zone Electron Environment," NSSDC 72-06, August 1972.

2. Michael J. Teague and James I. Vette, "The Inner Zone Electron Model AE-5," NSSDC 72-10, November 1972.

3. Michael J. Teague and James I. Vette, "A Model of the Trapped Electron Population for Solar Minimum," NSSDC 74-03, April 1974.

4. James I. Vette, Antonio B. Lucero, and Jon A. Wright, "Models of the Trapped Radiation Environment; Volume II: Inner and Outer Zone Electrons," NASA SP-3024, 1966.

5. James I. Vette and Antonio B. Lucero, "Models of the Trapped Radiation Environment; Volume III: Electrons at Synchronous Altitudes," NASA SP-3024, 1967.

6. Michael J. Teague and E. G. Stassinopoulos, "A Model of the Starfish Flux in the Inner Radiation Zone," GSFC X-601-72-487, December 1972.

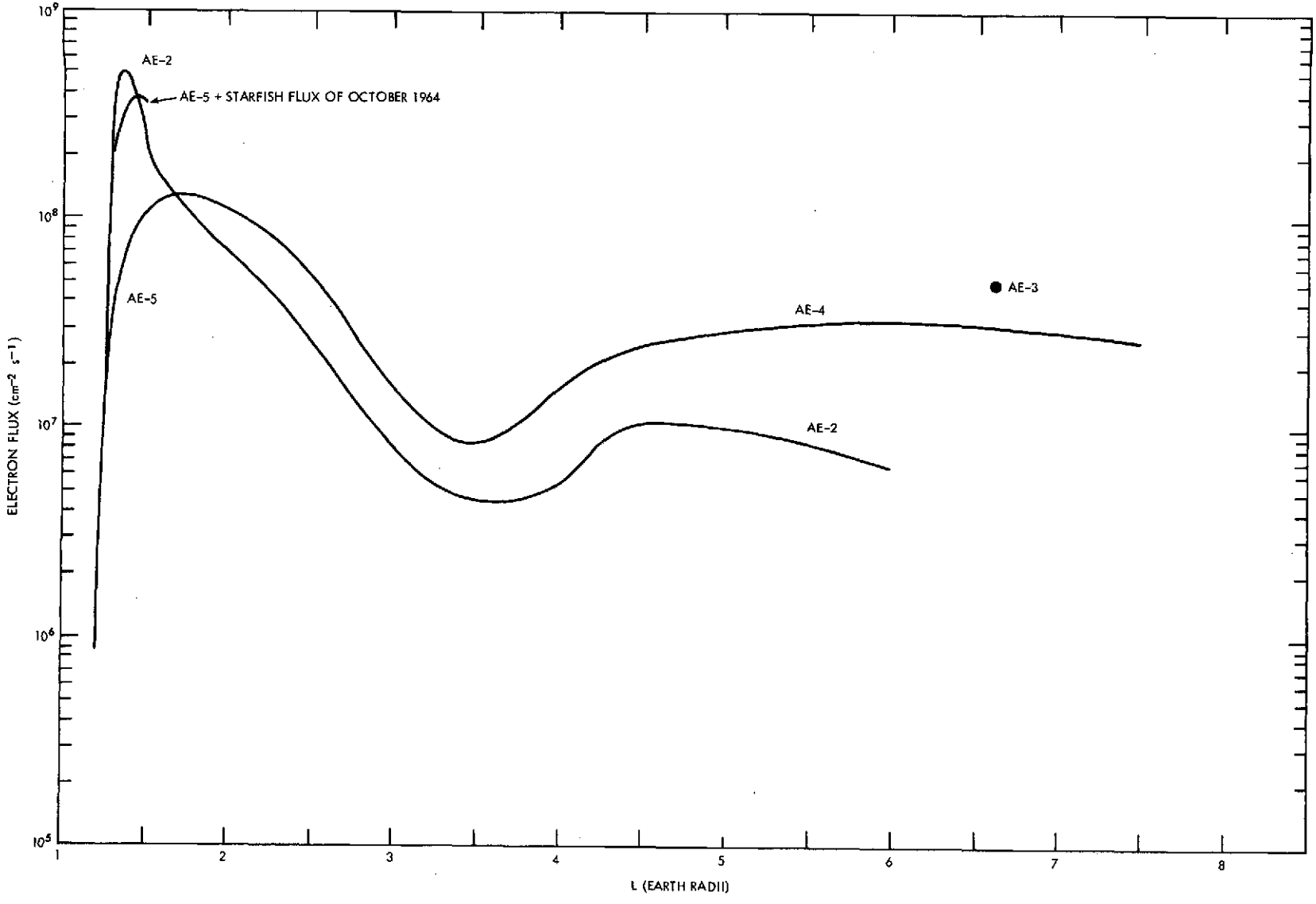

Figure 1. Radial Profile of Omnidirectional Equatorial Flux of Electrons with Energies Above 0.04 MeV Near Solar Minimum

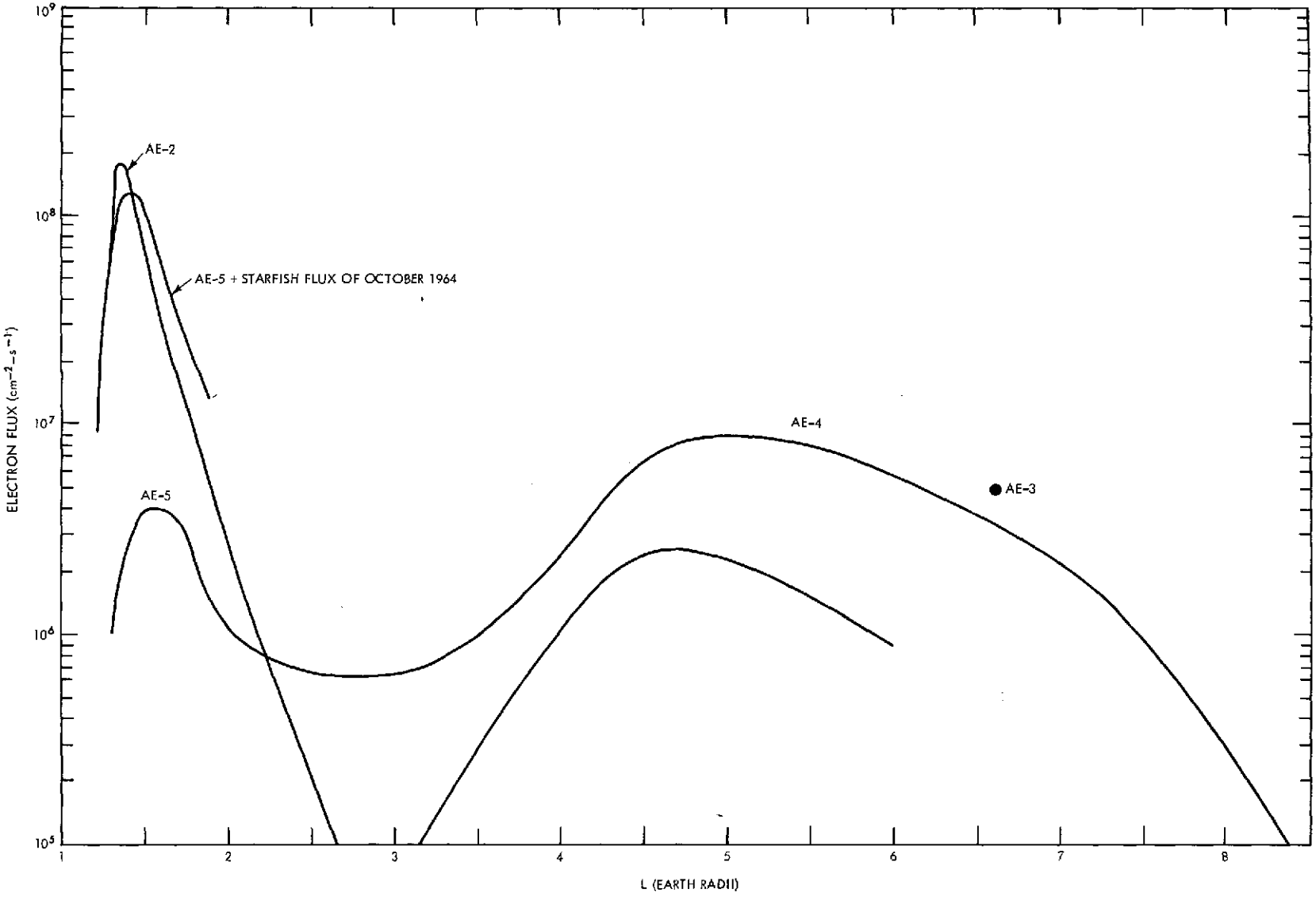

Figure 2. Radial Profile of Omnidirectional Equatorial Flux of Electrons with Energies Above 0.5 MeV Near Solar Minimum

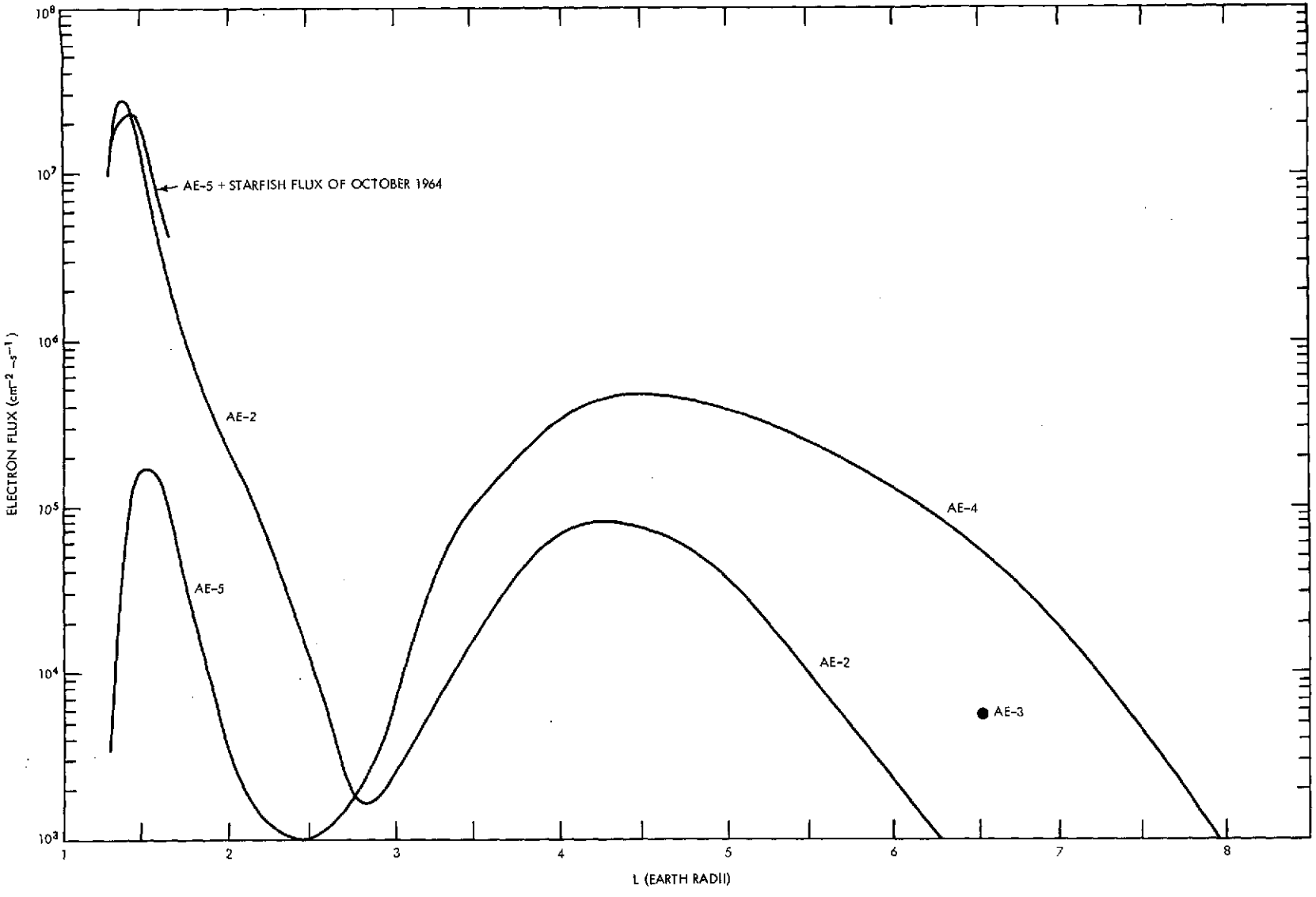

Figure 3. Radial Profile of Omnidirectional Equatorial Flux of Electrons with Energies Above 2 MeV Near Solar Minimum

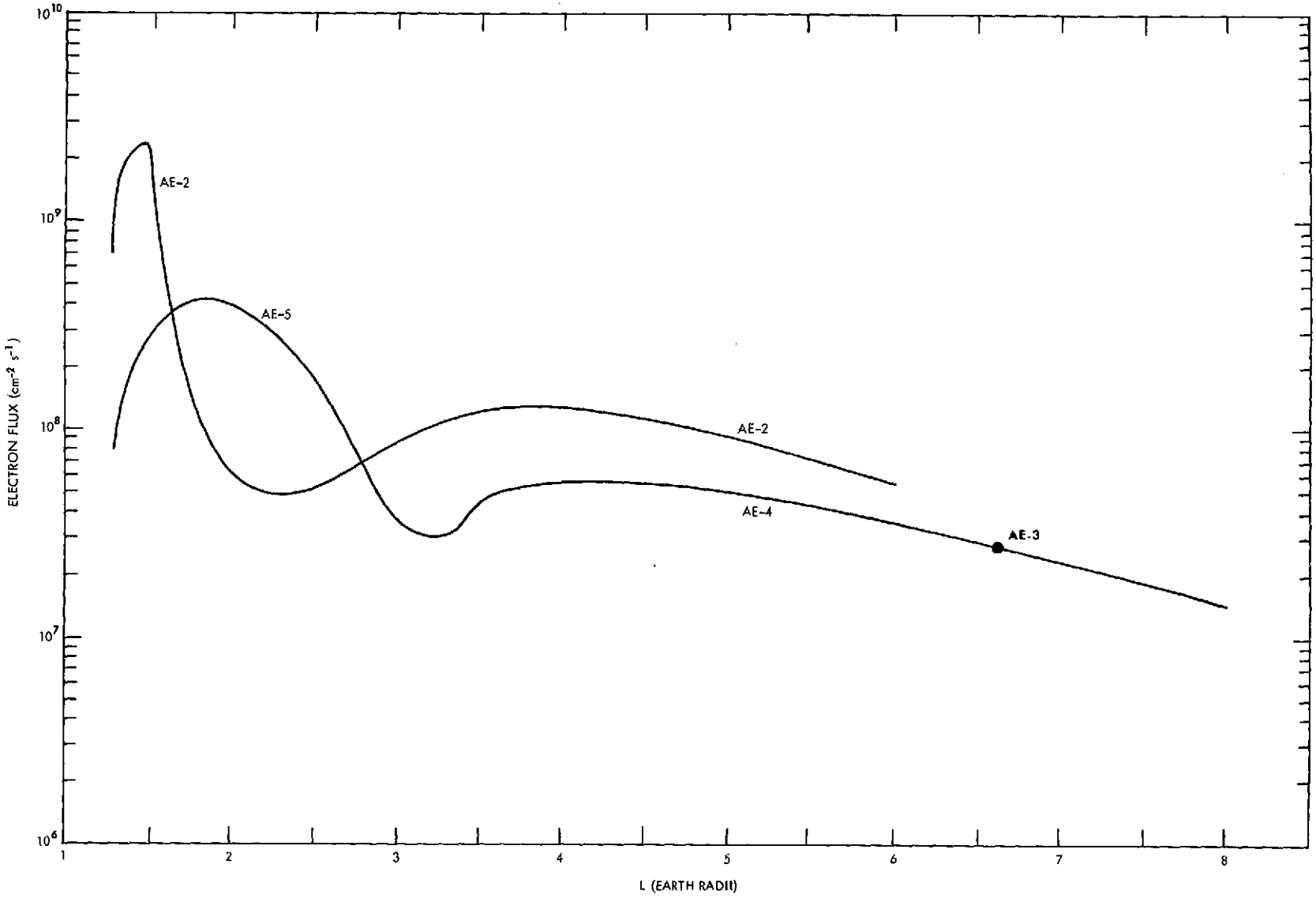

Figure 4. Radial Profile of Omnidirectional Equatorial Flux of Electrons with Energies Above 0.04 MeV Near Solar Maximum

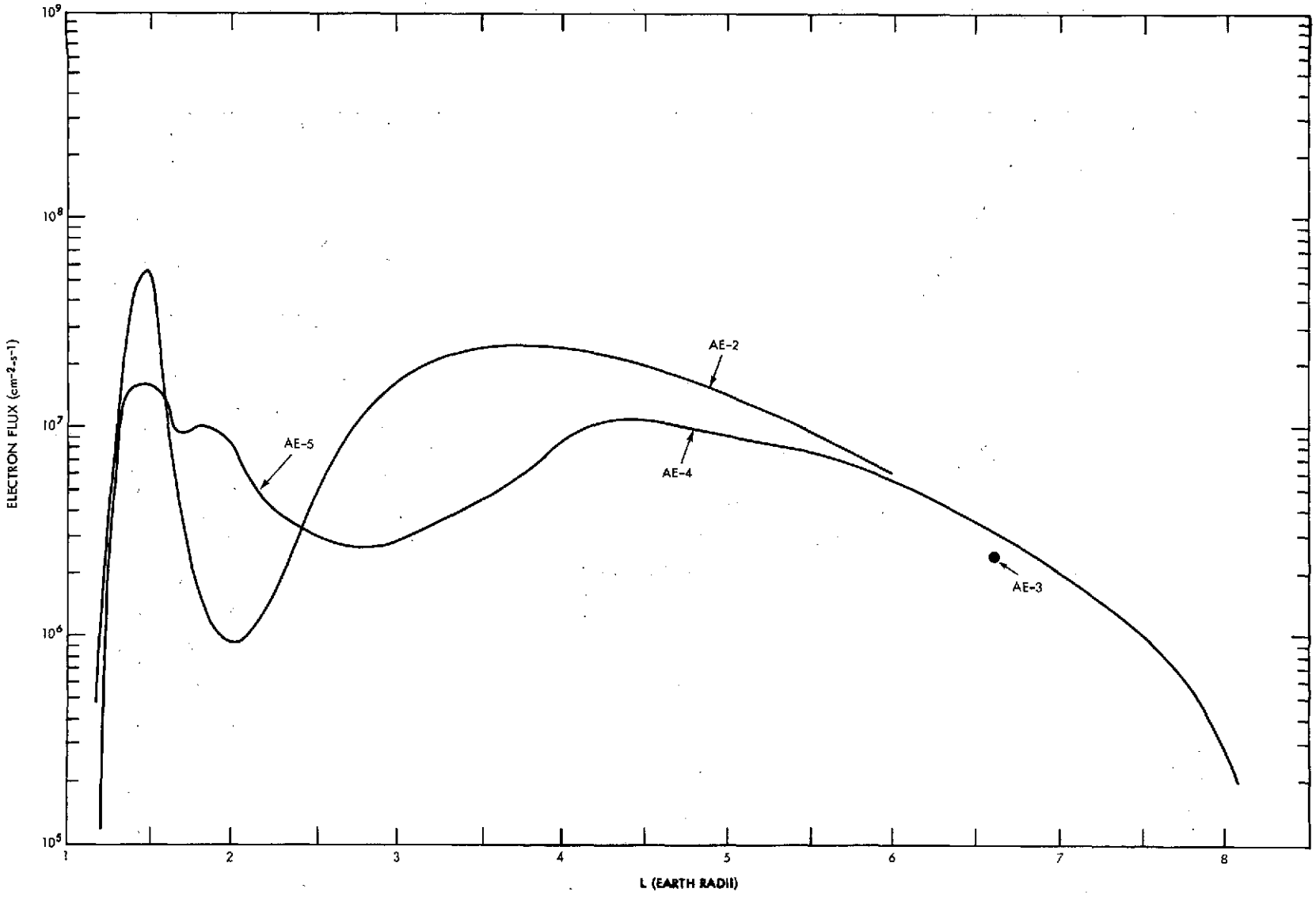

Figure 5. Radial Profile of Omnidirectional Equatorial Flux of Electrons with Energies Above 0.5 MeV Near Solar Maximum

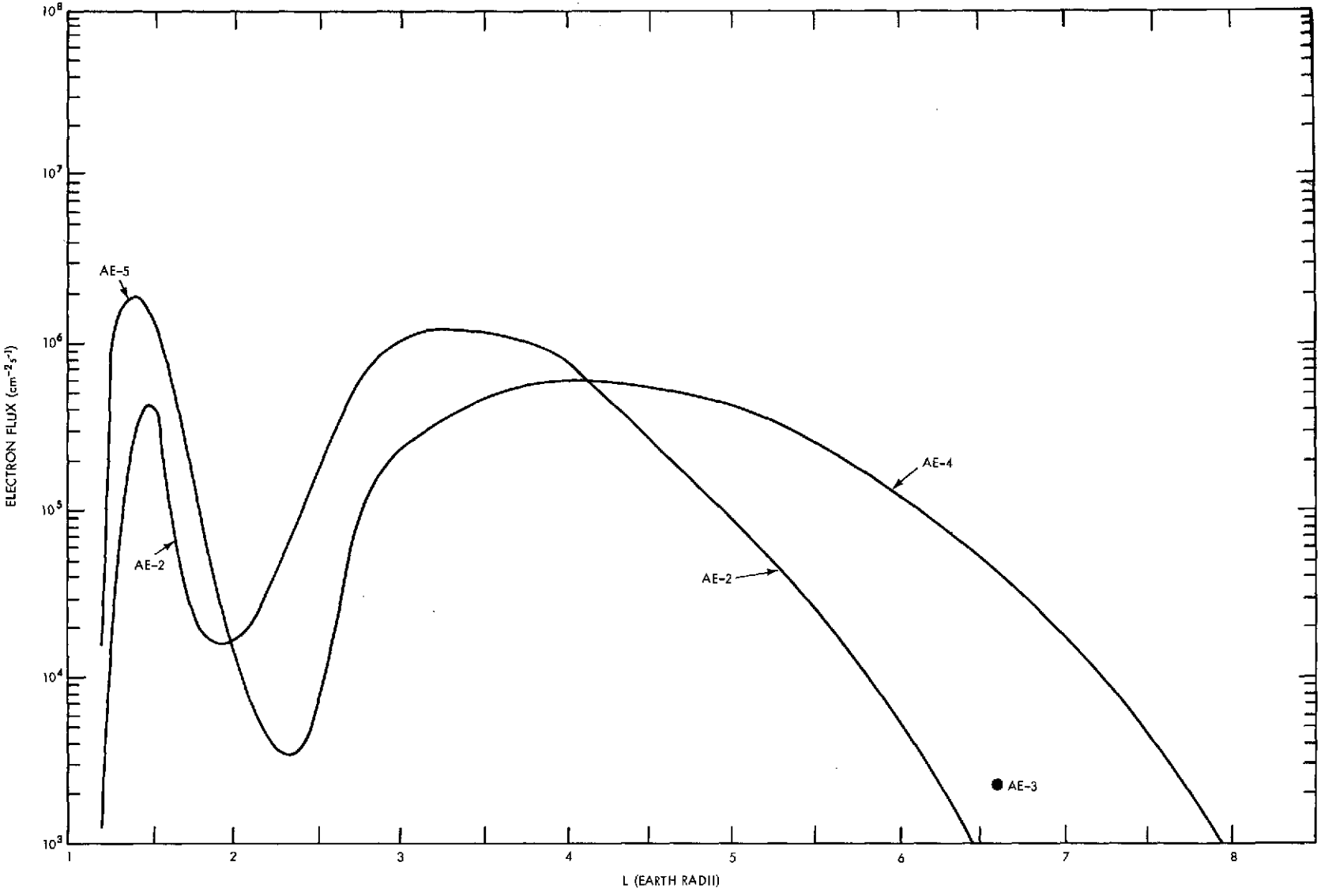

Figure 6. Radial Profile of Omnidirectional Equatorial Flux of Electrons with Energies Above 2 MeV Near Solar Maximum

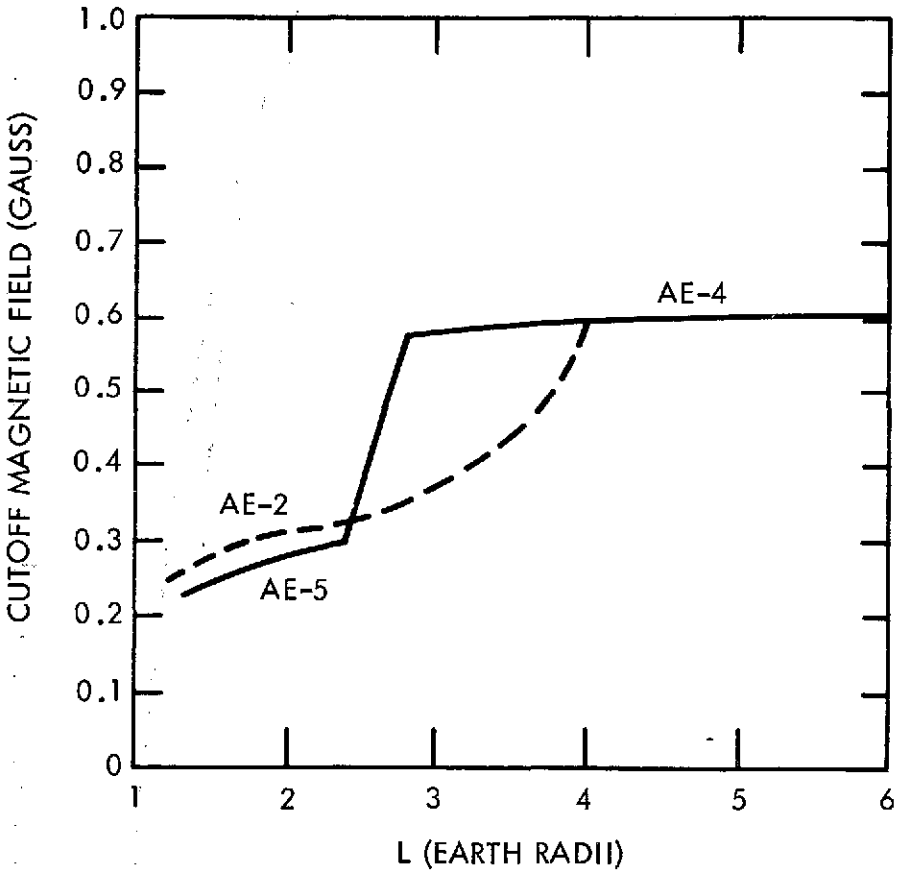

Figure 7. Comparison of the Cutoff Magnetic Field Used in AE-4 and AE-5 with AE-2 as a Function of L

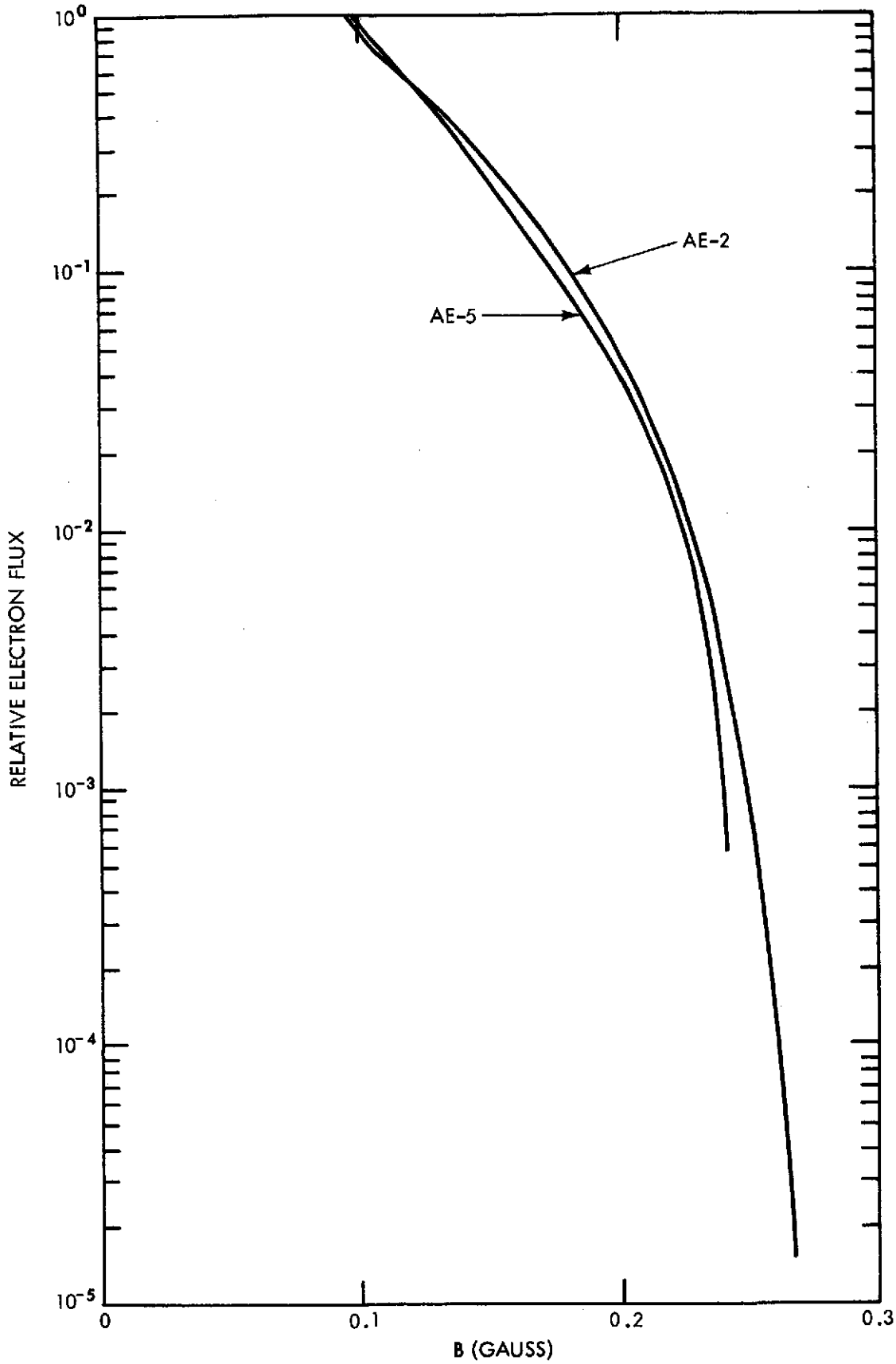

Figure 8. Dependence of Omnidirectional Electron Flux on Magnetic Field Intensity for L = 1.5 Earth Radii

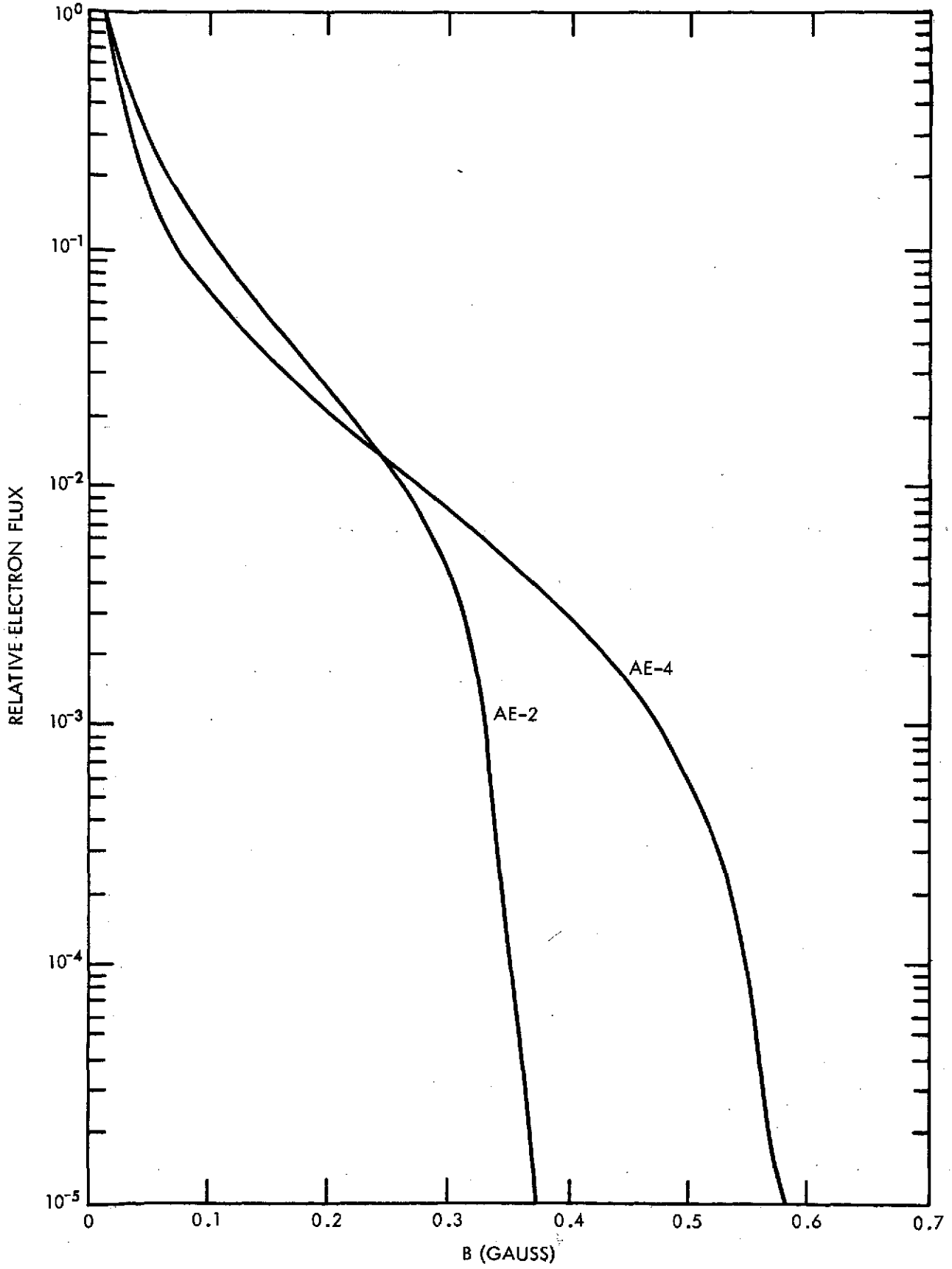

Figure 9. Dependence of Omnidirectional Electron Flux on Magnetic Field Intensity for L = 3.0 Earth Radii

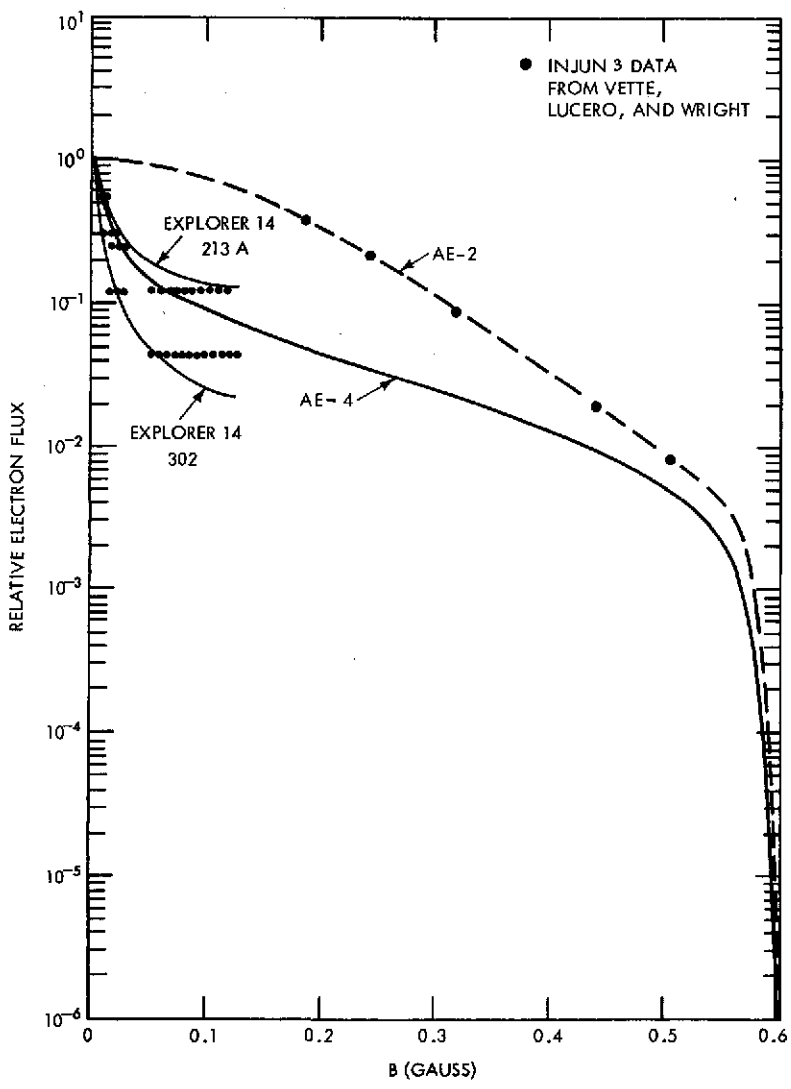

Figure 10a. Dependence of Omnidirectional Electron Flux on Magnetic Field Intensity for L = 5.0 Earth Radii for AE-2 and AE-4

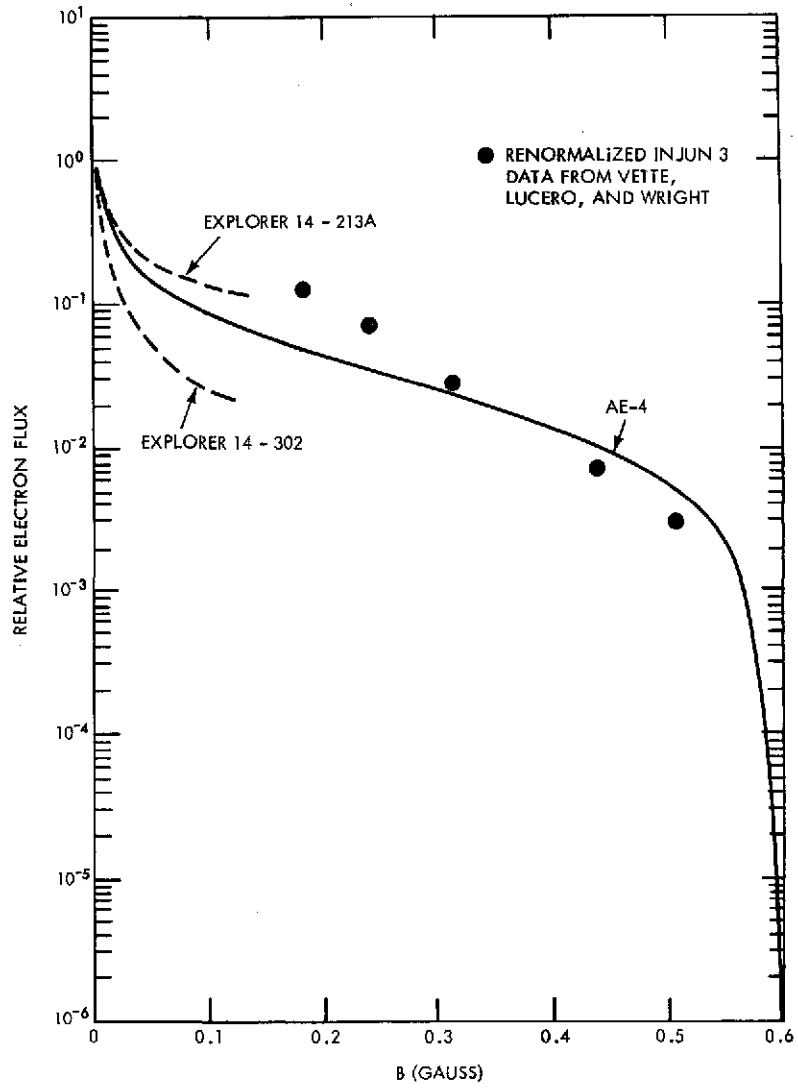

Figure 10b. AE-4 Dependence of Omnidirectional Electron Flux on Magnetic Field Intensity for L = 5.0 Earth Radii

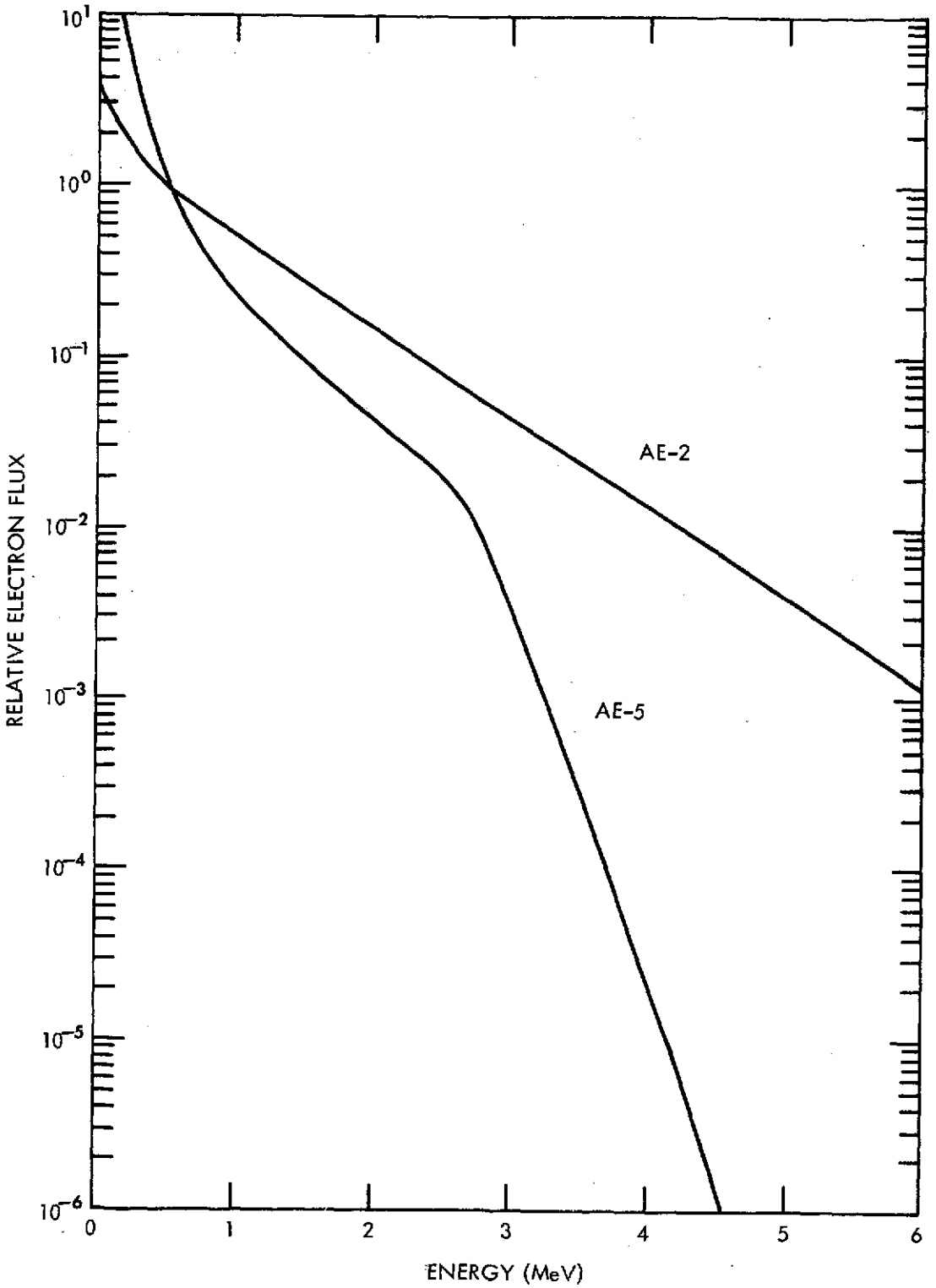

Figure 11. Equatorial Omnidirectional Integral Spectrum of Electrons at L = 1.5 Earth Radii, Normalized to Unity at 0.5 MeV

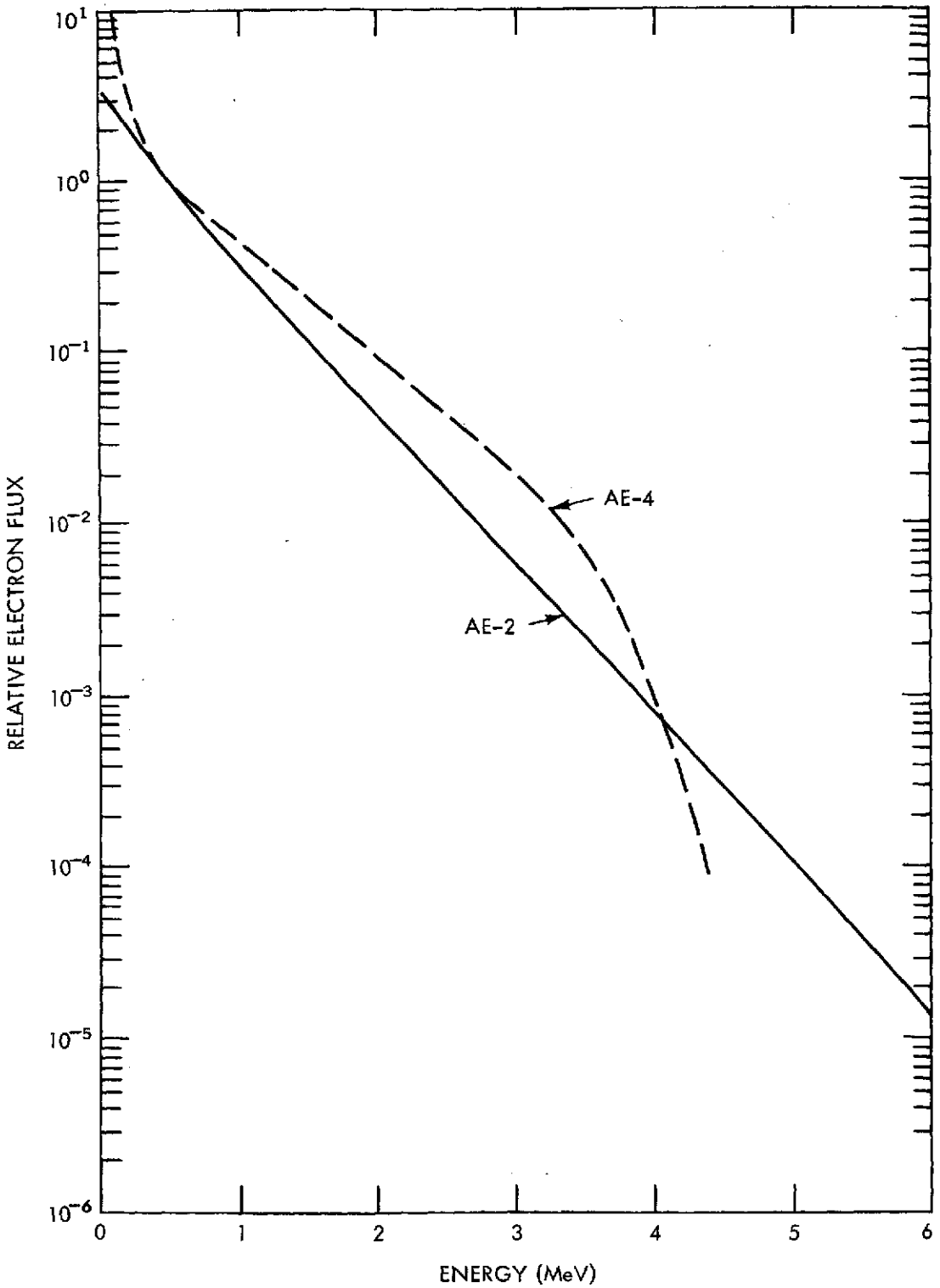

Figure 12. Equatorial Omnidirectional Integral Spectrum of Electrons at L = 3.0 Earth Radii, Normalized to Unity at 0.5 MeV

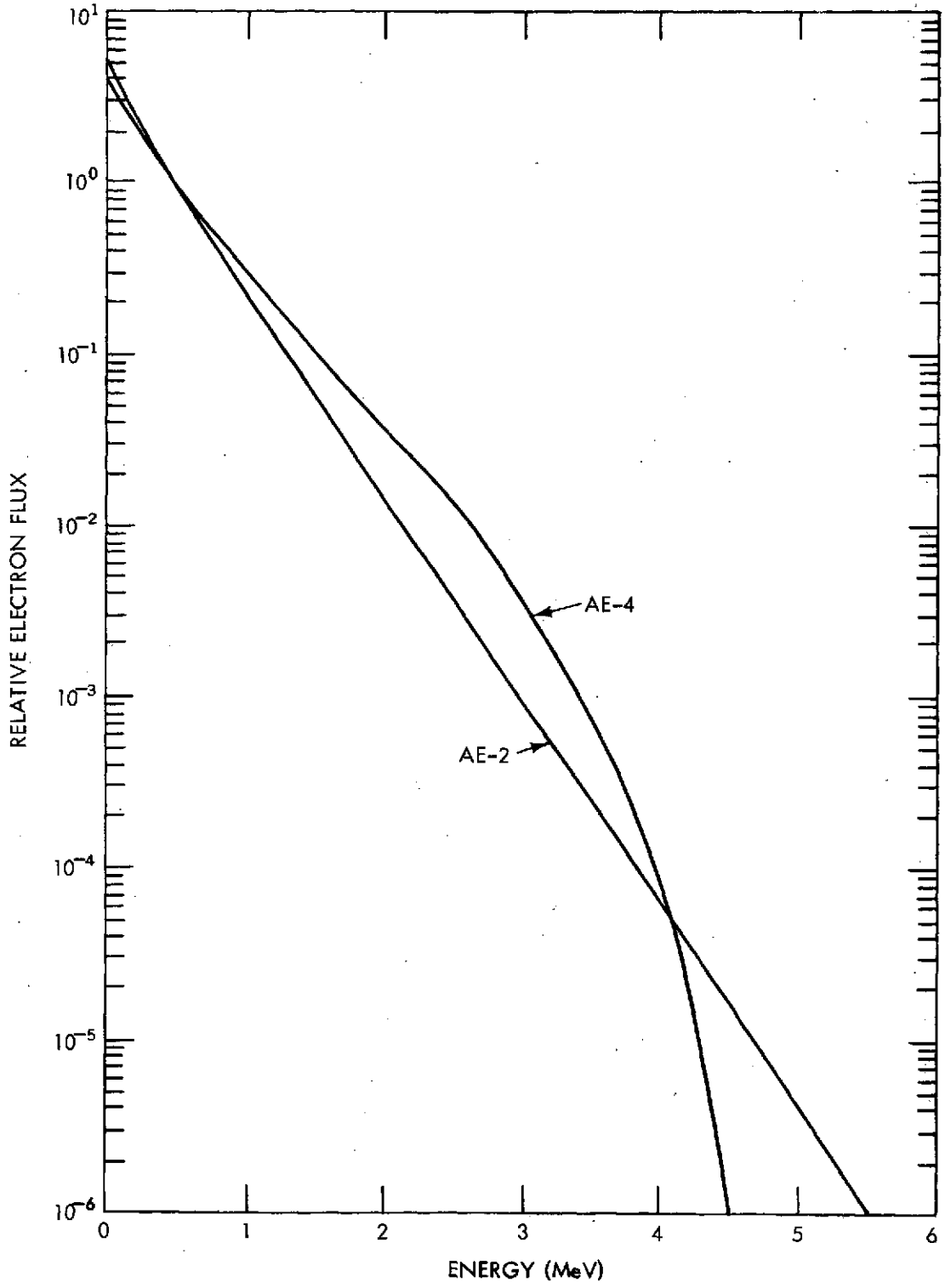

Figure 13. Equatorial Omnidirectional Integral Spectrum of Electrons at L = 5.0 Earth Radii, Normalized to Unity at 0.5 MeV

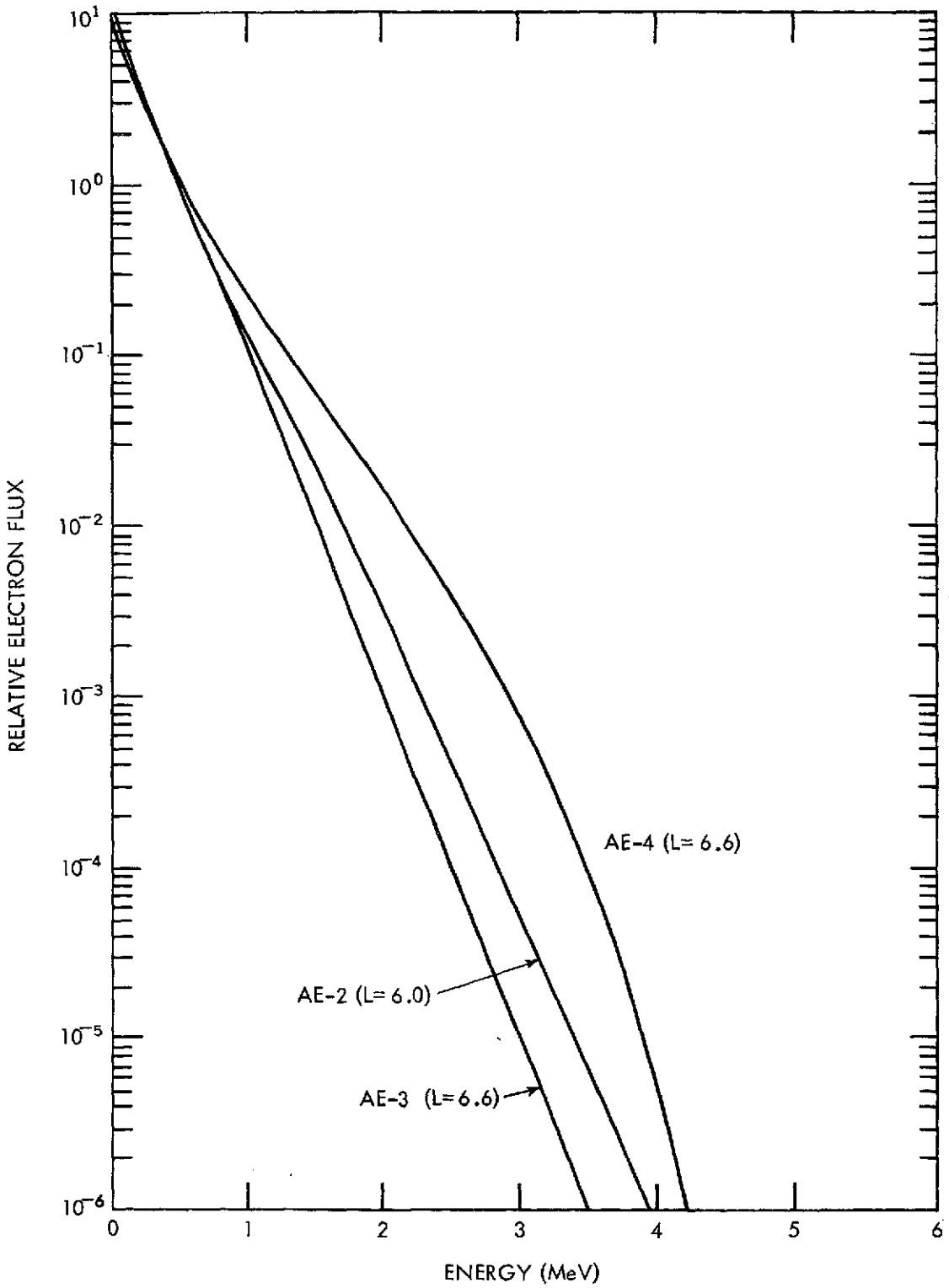

Figure 14. Equatorial Omnidirectional Integral Spectrum of Electrons at L = 6.6 and 6.0 Earth Radii, Normalized to Unity at 0.5 MeV

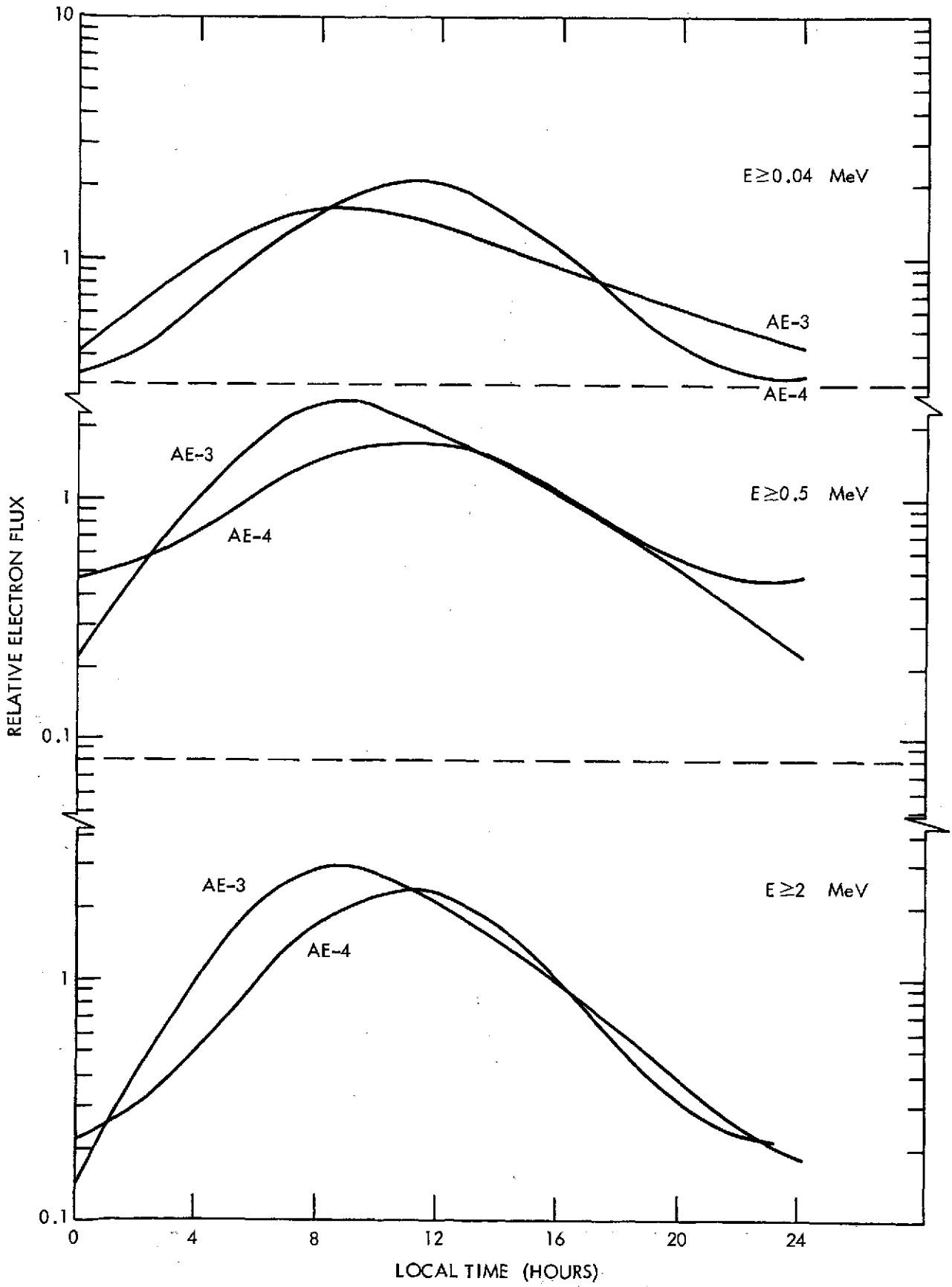

Figure 15. Local Time Dependence of Flux for AE-3 at L = 6.6 Earth Radii and AE-4 at L = 6.5 Earth Radii

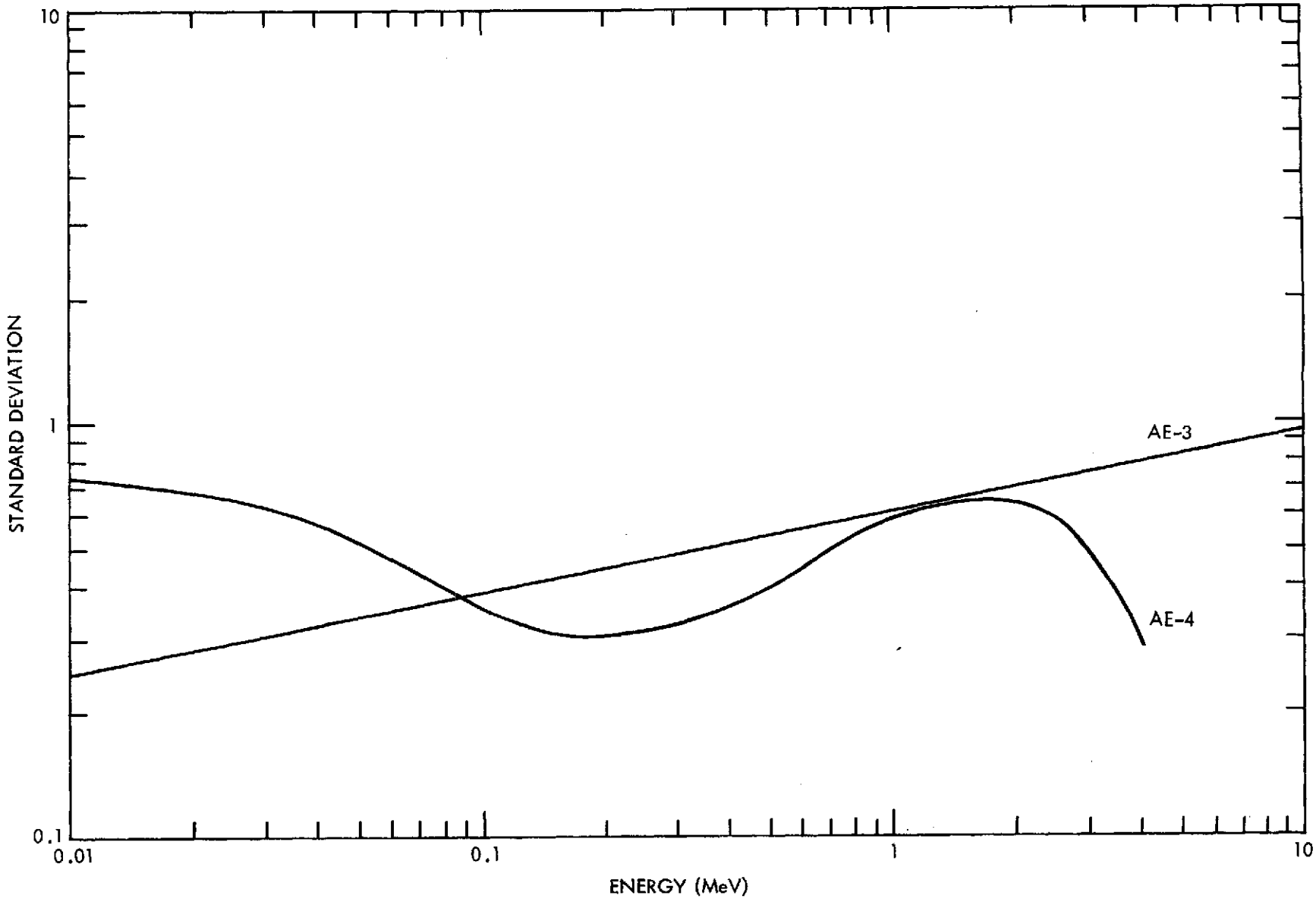

Figure 16. Standard Deviation for Log-Normal Statistical Functions for AE-3 at L = 6.6 Earth Radii and AE-4 at L = 6.5 Earth Radii

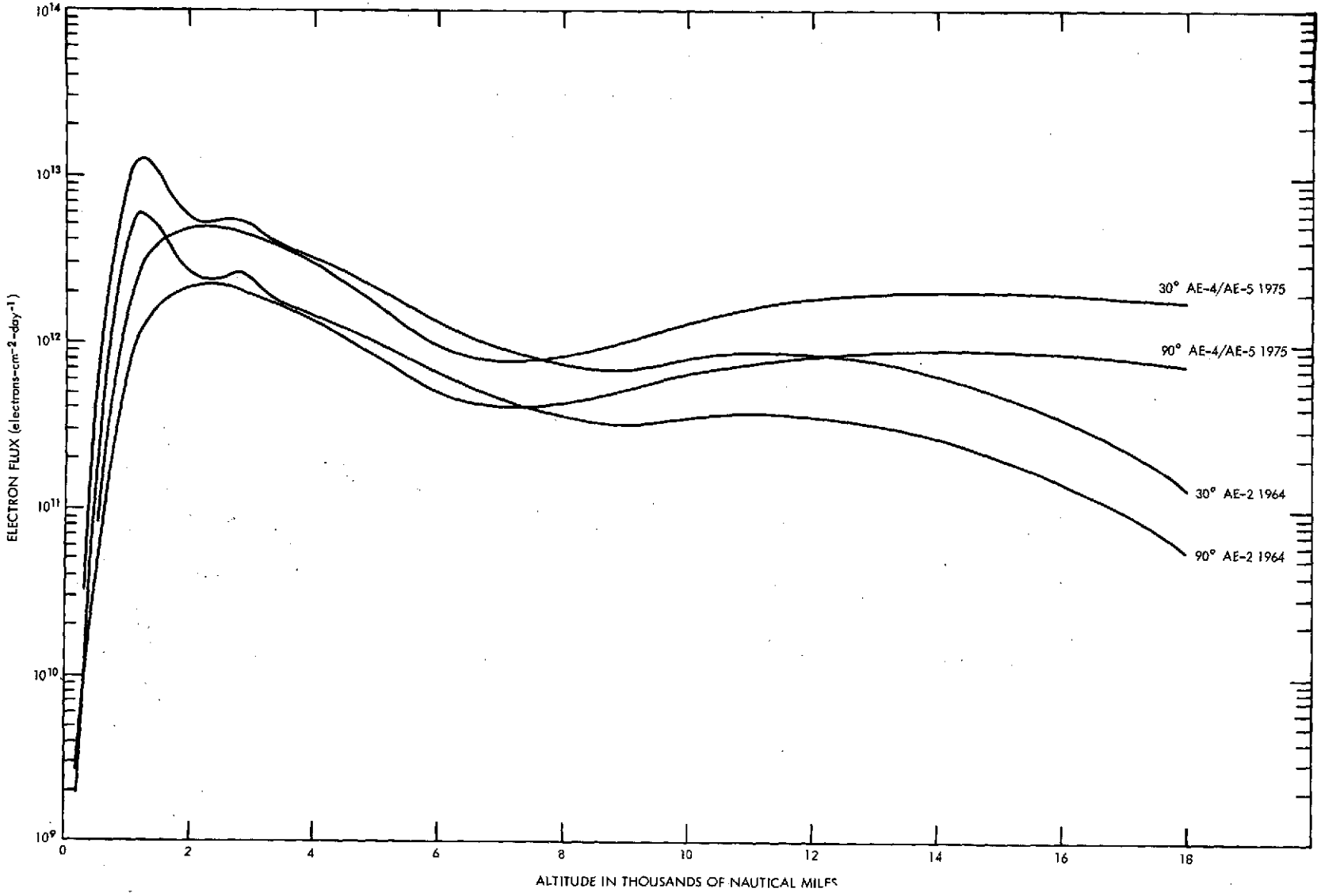

Figure 17. Comparison of Orbit Integrations for 50 keV Electrons Near Solar Minimum

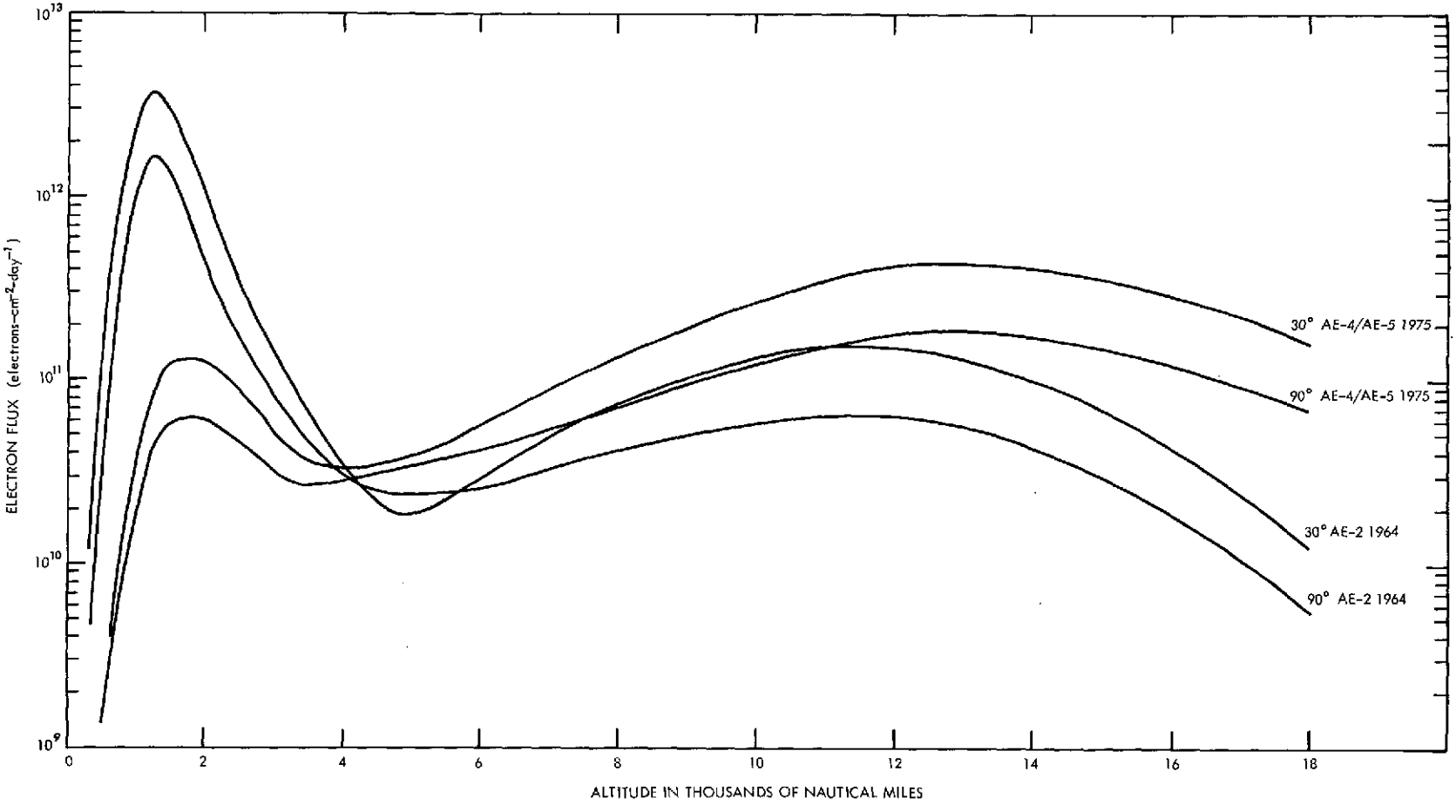

Figure 18. Comparison of Orbit Integrations for 0.5 MeV Electrons Near Solar Minimum

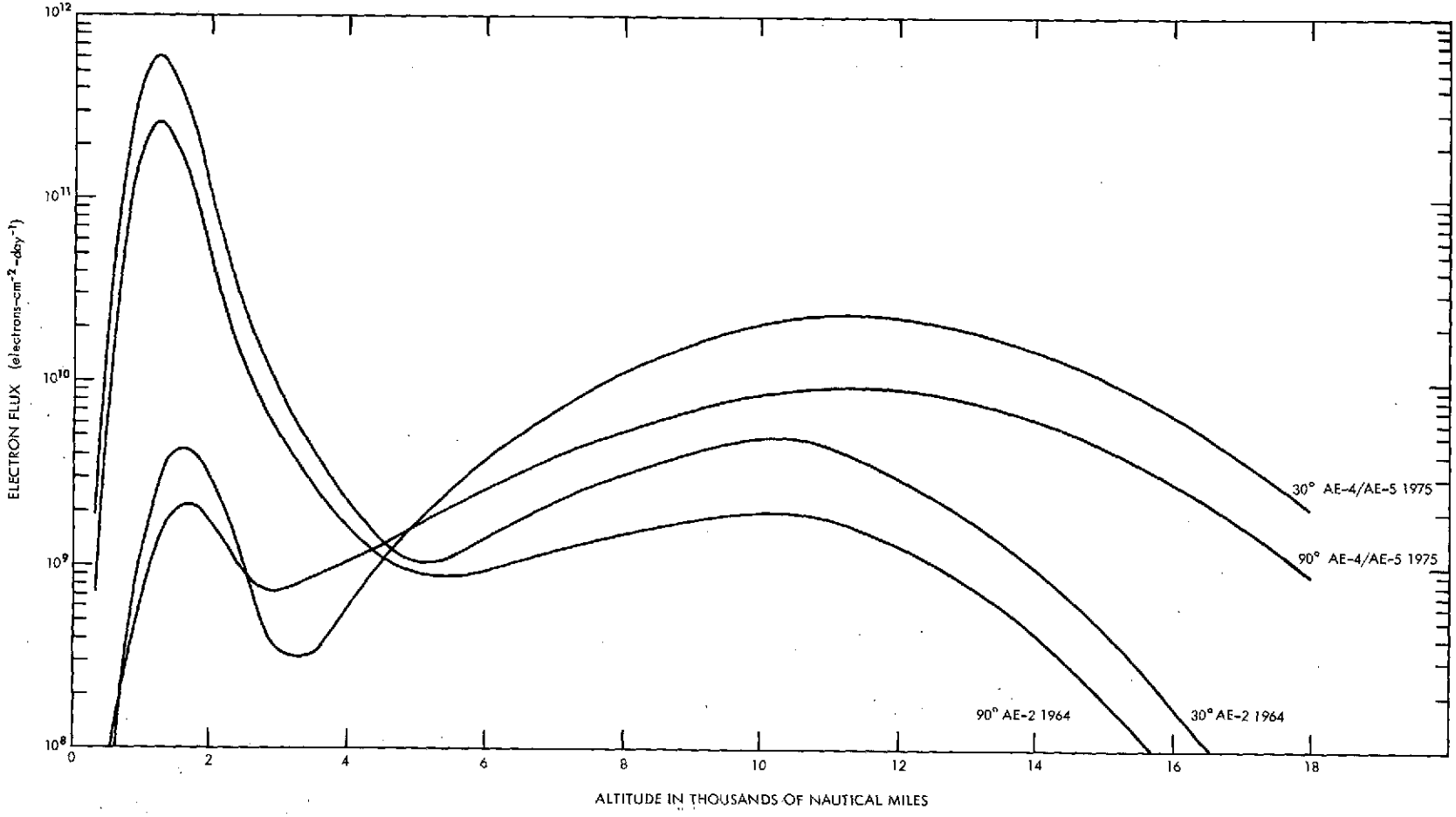

Figure 19. Comparison of Orbit Integrations for 2 MeV Electrons Near Solar Minimum

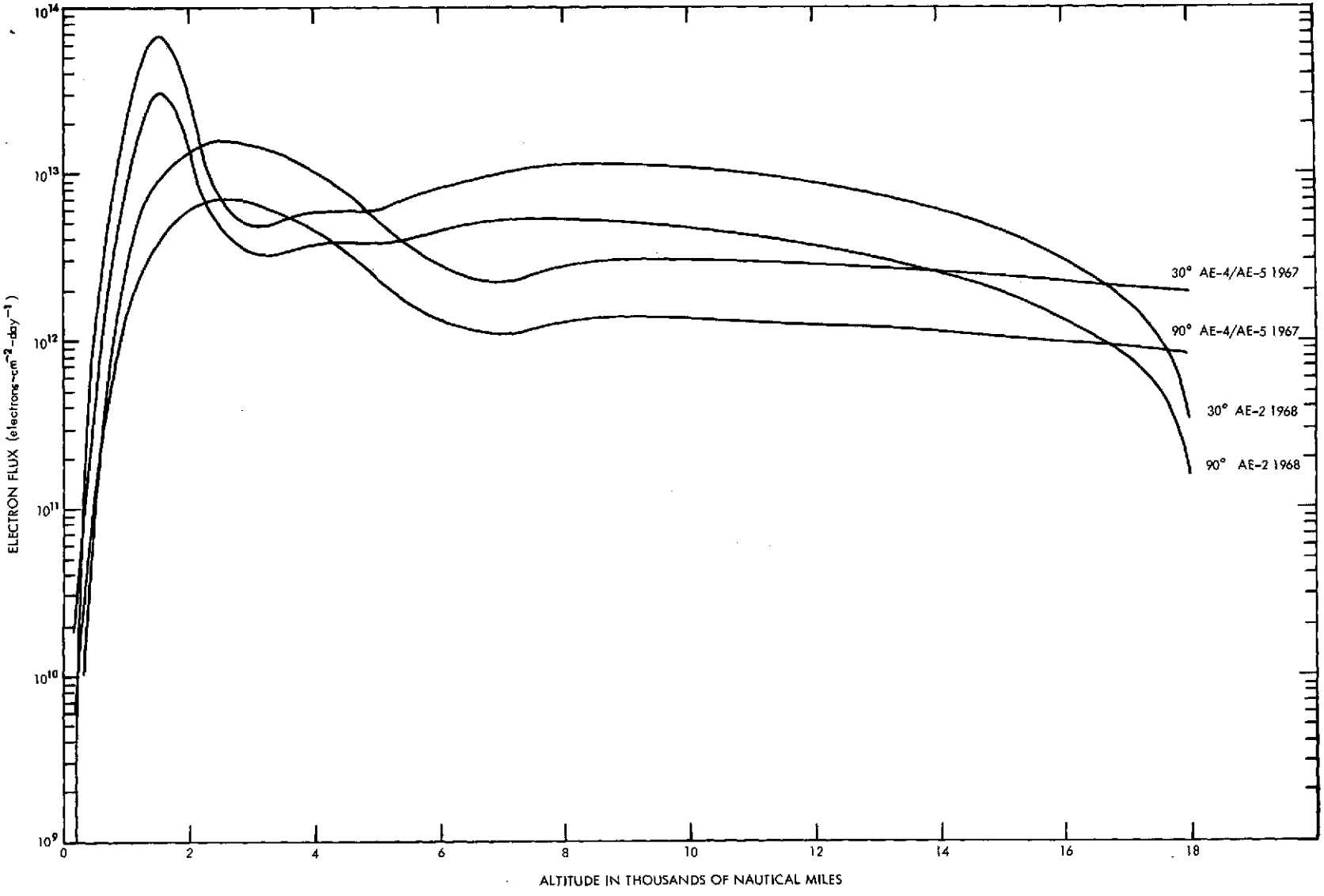

Figure 20. Comparison of Orbit Integrations for 50 keV Electrons Near Solar Maximum

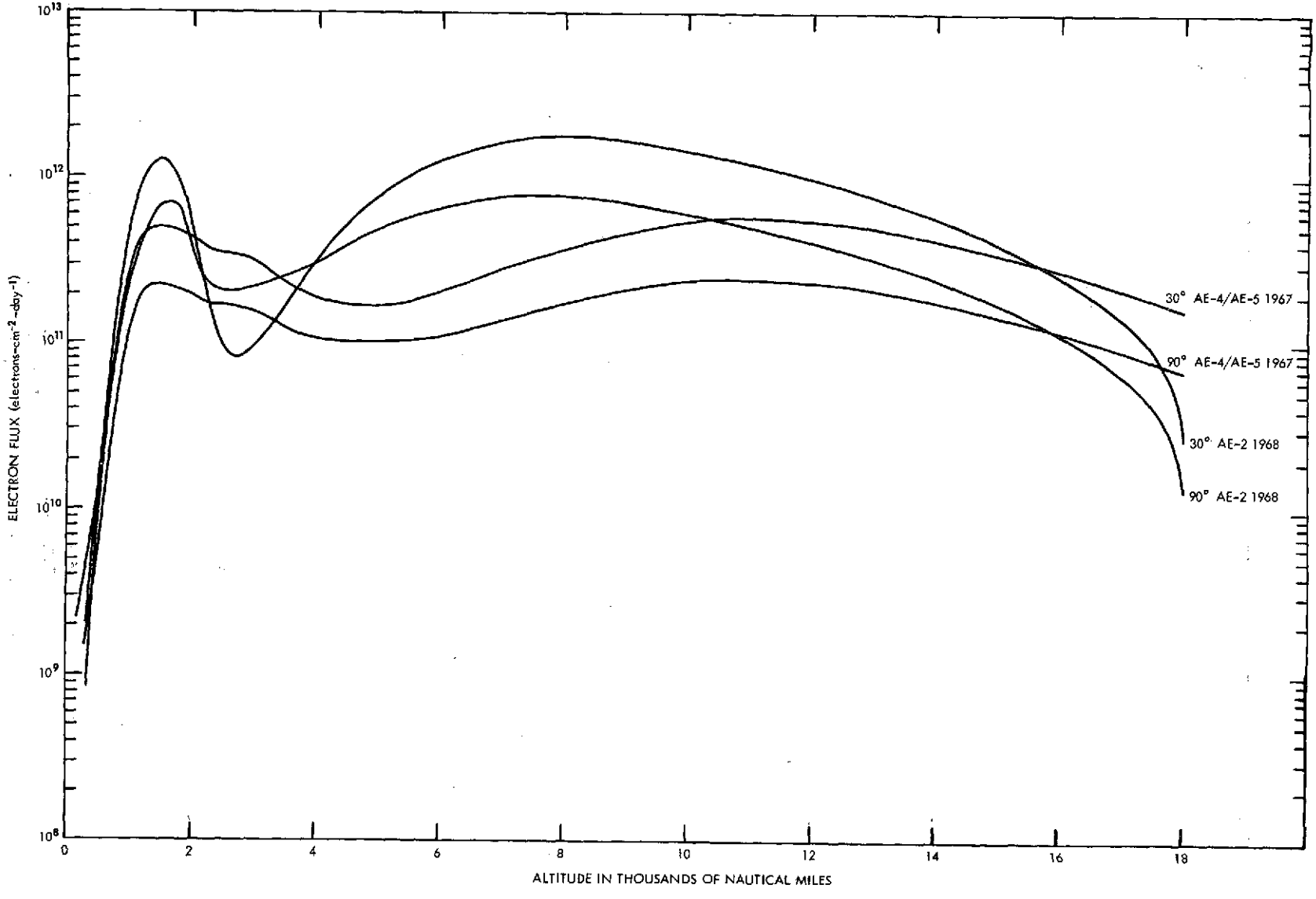

Figure 21. Comparison of Orbit Integrations for 0.5 MeV Electrons Near Solar Maximum

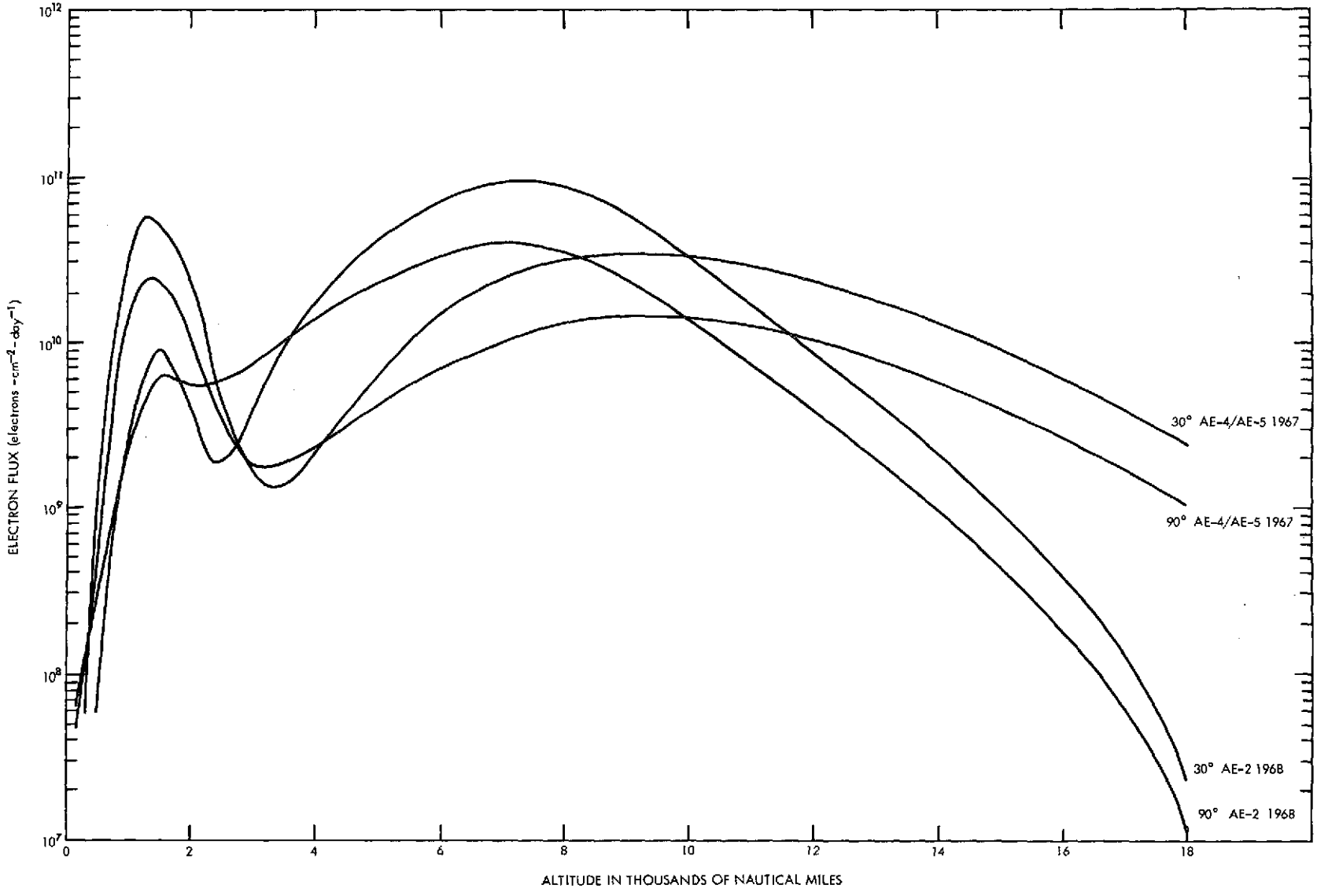

Figure 22. Comparison of Orbit Integrations for 2 MeV Electrons Near Solar Maximum